Green Hydrogen Production Using a Low-Cost HHO Generator: Design, Fabrication, and Performance Analysis

Fawad Khan, Arshad Ali Khan, Zarar Khan, Muhammad Hamza, Abu Zar, Ahsan Khan, Faryal Khan

Department of Mechanical Engineering, University of Engineering and Technology Peshawar, Peshawar, 25120, Pakistan

*__Correspondence:__ engrarshad@uetpeshawar.edu.pk

Citation | Khan.F, Khan.A.A, Khan.Z, Hamza.M, Zar.A, Khan.A, Khan.F," Green Hydrogen Production Using a Low-Cost HHO Generator: Design, Fabrication, and Performance Analysis",IJIST Vol. 8 Issue. 6 pp 2531-2550, September 2026

DOI: https://doi.org/10.33411/IJIST/2020

Received | Aug 18, 2026 **Revised |** Aug 31, 2026 **Accepted |** Sep 05, 2026 **Published |** Sep 08, 2026.

Green hydrogen is seen as one of the few viable routes to decarbonizing sectors that are difficult to electrify directly, but high capital and catalyst costs still put a working electrolyzer out of reach for many smaller laboratories and developing economies. This paper reports the design, fabrication, and performance characterization of a low-cost HHO Generator that produces hydrogen through alkaline water electrolysis, using bare, uncatalyzed SS-316L stainless-steel bipolar electrodes in a 30 wt% aqueous NaOH electrolyte (70:30 v/v tap-water-to-NaOH stock mixture). The system integrates a closed electrolyte circulation loop, a gas–water separator, and a low-pressure hydrogen storage vessel; the complete assembly was modeled in SolidWorks prior to fabrication to verify sealing and fastener alignment before any metal was cut. Under a fixed 12 V, 22 A DC input, the finished unit produced hydrogen at a measured rate of 0.01 L/s (0.6 L/min), corresponding to an electrical input power of 264 W and a recovered hydrogen energy output of 108 W (lower heating value basis), for an overall system efficiency of 41%. This is below the 65–75% typical of commercial alkaline electrolyzers and the 70–82% typical of PEM systems, consistent with the expected penalty of omitting a catalyst coating entirely. All reported values reflect a single measurement run at one fixed operating point; repeat-trial statistics and formal measurement uncertainty were not part of the original test protocol, and this is stated explicitly here as a limitation rather than masked with unreported error bars. The central finding is that a complete, working hydrogen generator — electrode stack, circulation, separation, and storage — can be built end to end from components available in local Pakistani markets at a small fraction of commercial cost, providing a reproducible baseline for future catalyst-coating and design studies.

Keywords: Green Hydrogen, HHO Generator, Alkaline Water Electrolysis, SS-316L Electrodes, Hydrogen Production Rate, System Efficiency, Renewable Energy.

Introduction:

The world is not short of energy demand, and every year it grows a bit more than the year before it. Fossil fuels still meet most of that demand, and burning them keeps adding CO_2, CO, SO_x, and NO_x to the atmosphere, feeding climate change, sea-level rise, and the slow erosion of ecosystems that depend on a stable climate [1], [2]. The International Energy Agency puts global hydrogen demand at close to 100 million tonnes for 2024, and that figure is growing faster than energy demand overall — a sign of how central hydrogen has become to decarbonization plans, at least on paper. Hydrogen itself stores roughly 120 MJ/kg, nearly three times the energy density of gasoline by mass, and it only produces water vapor when it is burned or run through a fuel cell.

Whether that makes hydrogen "clean" depends entirely on where it comes from. Grey hydrogen, made by steam methane reforming without carbon capture, is still about 95% of global supply and carries a footprint of roughly 9–12 kg CO_2 per kilogram of hydrogen produced. Blue hydrogen bolts carbon capture onto the same process and claims an 85–90% cut in emissions, though once upstream methane leakage is counted, several life-cycle studies put its real footprint 20–40% higher than the headline number — useful as a bridge technology, but not a long-term answer. Green hydrogen, made by electrolysis running on renewable electricity, is the only one of the three with a genuinely low life-cycle footprint, and IRENA's 1.5 °C pathway calls for its output to go from almost nothing today to 125 million tonnes a year by 2030 [1].

Electrolysis itself is simple chemistry — split water at the cathode and anode:

Cathode: $2H_2O + 2e^- \rightarrow H_2 + 2OH^-$ Anode: $4OH^- \rightarrow O_2 + 2H_2O + 4e^-$

but turning that reaction into a deployable technology has produced four rather different families of electrolyzer, at four different stages of maturity. Alkaline water electrolysis (AWE) is the oldest and most commercially proven: a liquid KOH or NaOH electrolyte, nickel- or cobalt-based catalysts instead of precious metals, and service lives that regularly pass 90,000 hours [3]. Proton exchange membrane (PEM) systems trade that simplicity for speed and purity — faster response, cleaner gas — at the cost of platinum and iridium catalysts, and iridium in particular is scarce enough that several authors now treat it as a hard ceiling on how far PEM can scale [4], [5]. Anion exchange membrane (AEM) electrolysis is the newer attempt to get PEM's compact, membrane-based architecture without the precious-metal catalyst bill, though membrane durability under sustained alkaline conditions is still very much an open problem [6],[7],[8]. Solid oxide electrolysis (SOE) sits at the far end, running at 700–900 °C with the best theoretical efficiency of the four, but also the steepest materials and thermal-cycling challenges, which keeps it largely confined to pilot-scale demonstrations for now, and general treatments of water-electrolysis methodology place it alongside the other three as one coherent family of technologies rather than a separate field [9], [10].

Cost is really where these technologies pull apart from each other. Green hydrogen currently runs USD 4–8/kg against roughly USD 1–2/kg for grey hydrogen, and most of that difference comes down to electrolyzer capital cost and catalyst material rather than the electricity itself [11]. That is precisely why AWE's reliance on cheap, non-precious-metal catalysts matters so much — it is one of the few electrolysis routes where the catalyst bill does not dominate the economics [12]. What is missing from most of this literature, though, is the practical end of the problem: electrolyzer systems that a university lab, or a small research group in a country without a domestic electrolyzer industry, could actually build and characterize themselves. Commercial units are engineered for industrial deployment. They are not meant to be opened up, modified, or used to teach the electrochemistry underneath them [3]. Pakistan is a useful example of exactly this gap: the country has well-documented structural barriers to renewable energy deployment generally [13], yet has real, quantified potential for a

domestic green-hydrogen economy if that gap is addressed [14] — which is part of why a locally buildable electrolyzer platform is more than just a classroom exercise here.

A growing body of recent work has started to fill in the practical, low-cost end of this literature. Okonkwo et al. examined how electrode spacing affects hydrogen output in a home-made alkaline electrolyzer, finding that closer spacing measurably improved production rate at fixed voltage [15], and a companion study from the same group compared SS-316L against carbon-steel electrodes in an equivalent home-built cell, confirming SS-316L as the better-performing, corrosion-resistant, non-precious-metal choice [16]. Bunge et al. built and characterized a six-cell dry-cell oxyhydrogen prototype from low-cost components, reporting gas composition and efficiency for a fully DIY system [17]. More recently, Mousa et al. examined how applied voltage and electrolyte concentration affect a simple oxy-hydrogen generator's energy-conversion efficiency [18], Gad et al. built a wet-cell SS-316L electrolyzer with 136.5 cm^2 electrodes at a 4 mm plate spacing and tested both KOH and NaOH electrolytes across a concentration sweep, reporting a peak efficiency of 69.3% at 10 g/L NaOH and 18 A [19], and Fayez et al. optimized electrode area, plate configuration, and electrolyte concentration across four wet-cell configurations, with their best design reaching 59.74% overall efficiency [20]. These studies establish that catalyst-free, stainless-steel alkaline electrolyzers are a genuinely active and recent research area — but nearly all of them optimize a single cell in isolation, sweeping voltage or electrolyte concentration to chase peak efficiency, rather than reporting a complete, integrated system — circulation, gas–water separation, and storage included — built and characterized as a whole from parts available in a specific local market.

That gap is where this project sits. The HHO Generator is a laboratory-scale alkaline water electrolysis unit assembled from parts available in local Pakistani markets, using bare SS-316L stainless-steel electrodes with no catalyst coating at all. We are not claiming a breakthrough in the electrochemistry itself; the reaction is standard alkaline electrolysis, and the loss mechanisms we see are the well-documented ones — activation overpotential, ohmic resistance in the electrolyte, and gas-bubble blocking at the electrode surface [21], [22]. It is worth reporting that a complete, working system — electrode stack, electrolyte circulation, gas separation, storage — can be built end to end from locally sourced components at a small fraction of commercial cost, and characterized well enough to be genuinely useful as a research and teaching platform rather than a demonstration piece that only runs once.

Novelty and Research Contribution:

It is worth being direct about where this work does, and does not, advance on the recent literature just reviewed. On efficiency alone, this system's 41% sits below the 59.74% reported by Fayez et al.'s optimized wet-cell design [20] and the 69.3% reported by [19], both of which swept electrode configuration or electrolyte concentration to find a best-case operating point. This system was tested at a single fixed condition, with no such optimization sweep, which accounts for a meaningful part of that gap.

The contribution here is narrower and, we think, still useful: this is a complete, closed-loop system — electrolyte circulation, gas–water separation, low-pressure storage, and a water-displacement measurement chain — built and characterized as one integrated unit, rather than an isolated electrode-pair test in a beaker. Most of the directly comparable low-cost studies [15][16][17][18][19][20] report cell-level results only, without a downstream separation and storage train; this paper documents that full chain, component by component, with sourcing information specific to the Pakistani market, so that the build is reproducible by another university lab working under similar resource constraints. In that sense the intended contribution is less about beating the efficiency numbers in Table 4 and more about providing an honestly characterized, fully documented reference system — including its unresolved inconsistencies and unmeasured parameters, flagged explicitly rather than smoothed over —

that a future study, including our own follow-on catalyst work, can build on and directly improve.

Research Objectives:

1. The work reported here was carried out against ten specific objectives, each cross-referenced below to the section in which it is addressed:
2. Design and fabricate a complete, functioning electrolyzer for green hydrogen production via alkaline water electrolysis.
3. Use only locally available, cost-effective, corrosion-resistant materials throughout construction.
4. Document the alkaline electrolyzer's actual behavior — the electrode reactions, the electrolyte, and how the gases separate.
5. Investigate ways to raise hydrogen output through electrode material and catalyst-coating choices.
6. Characterize the voltage–current behavior and overall performance of the finished system.
7. Calculate the hydrogen production rate along with the Faradaic and energy efficiency.
8. Study electrolyte circulation, gas separation, and temporary hydrogen storage.
9. Develop and follow standard start-up, testing, and emergency-shutdown procedures.
10. Assess the market context and potential impact of alkaline-electrolysis green hydrogen production.

Materials and Methods:

Design Approach:

We followed a fairly standard Conceive–Design–Implement–Operate (CDIO) sequence. The first pass through the literature compared AWE, PEM, AEM, and SOE on cost, efficiency, and how easy each one would be to build with materials we could actually source, and alkaline water electrolysis came out ahead on all three counts — no precious-metal catalyst requirement, and a design simple enough to fabricate in a mechanical workshop rather than a cleanroom. Before any metal was cut, we modeled the full assembly in SolidWorks: the electrode stack, the sealing arrangement, the gas–liquid separator, and the support frame, together with rough calculations of electrode area, current density, and expected hydrogen output. Components were then sourced from markets in Peshawar, Rawalpindi, and Lahore, fabricated and assembled in the Mechanical Engineering Workshop, and tested under controlled conditions, with a leak check, an electrical check, and a flow-stability check built into every stage before moving to the next one.

System Architecture:

The HHO Generator operates as a closed loop rather than a static bath, primarily to keep the electrolyte moving rather than stagnating around the electrodes. The reservoir contains a 70:30 mixture of tap water and NaOH by volume (approximately 30 wt% NaOH), which provides the ionic conductivity required for the reaction; this is the sole electrolyte used throughout the reported testing. A 12 V, 8 W DC submersible pump pulls this electrolyte from the reservoir through the electrode cell and back, which does two things at once: it keeps ion transport reasonably even across the electrode faces, and it clears gas bubbles that would otherwise sit there and add resistance.

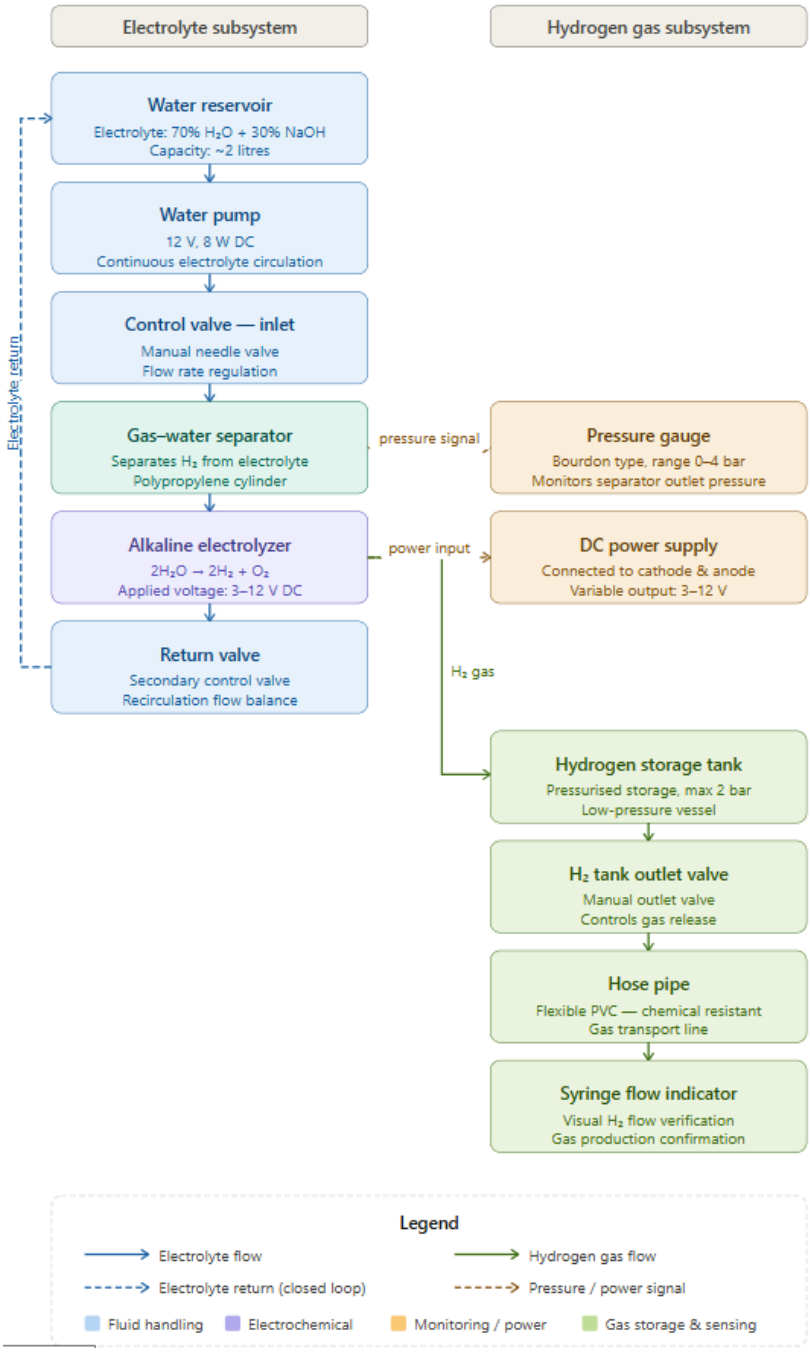

Figure 1. Process Flow Diagram of the HHO Generator System.

Figure 1 traces the complete pathway that gas and electrolyte follow through the system, from generation to storage. Starting at the reservoir:

The circulation pump draws electrolyte from the reservoir and delivers it to the electrode cell. Inside the cell, the applied DC voltage drives alkaline water electrolysis at the bipolar SS-316L plates, evolving hydrogen and oxygen gas directly into the circulating electrolyte stream.

The gas-laden electrolyte leaves the cell through an inlet control valve and enters the gas–water separator, where entrained droplets and moisture fall out under gravity.

Separated hydrogen gas continues on to the low-pressure storage vessel, monitored continuously by the pressure gauge at the separator outlet.

The de-gassed electrolyte returns to the reservoir through a second (return) control valve, closing the loop.

At the storage-tank outlet, a small syringe-based flow indicator provides simple visual confirmation that gas is still flowing during a run, while the same gas path feeds the water-displacement measurement described below.

Components and Specifications:

Table 1 lists the major components, their specifications, and where each one was sourced. Every choice here came down to three things: compatibility with the alkaline electrolyte, whether it was actually available locally, and cost relative to a student-project budget.

Table 1. Components and specifications of the HHO Generator.

Component	Specification	Source
DC power supply	Variable DC, 12 V, up to ~22–23 A	Karkhano Market, Peshawar
HHO Generator cell	SS-316L bipolar plates with NaOH electrolyte	Rawalpindi market
Electrolyte reservoir	HDPE tank, 5-litre capacity	Local hardware market, Peshawar
DC circulation pump	12 V, 8 W submersible pump	Local market, Peshawar
Flow control valves	Manual ball valves (1/4 inch)	Local plumbing market, Peshawar
Gas–water separator	Cylindrical separator vessel	Local market, Peshawar
Hydrogen storage tank	Pressurized cylinder, 2 bar rated	Local market, Peshawar
Pressure gauge	Bourdon-type, 0–10 mbar range	Lahore (ordered)
Connecting tubes	Silicone and PVC tubing	Khyber Bazaar Hardware, Peshawar
O-rings and seals	Rubber sealing gaskets	Local hardware market

One inconsistency is flagged here rather than quietly resolved: the power-supply rating recorded during component sourcing was 12 V, 17.5 A (210 W), while the operating condition actually used for the efficiency calculation is 12 V, 22 A (264 W). Both are kept exactly as they appear in the underlying project records; the 22 A figure is the one the reported results are calculated from, and the supply's true rated maximum current should be re-confirmed against its nameplate before any further submission.

Reproducibility Parameters:

Table 2 collects the specific build and operating parameters needed to reproduce this system, as requested in review. Several of these were not recorded as discrete, independently verified values in the underlying project documentation; those are marked accordingly rather than backfilled with assumed numbers.

Sizing these components mostly came down to two competing pulls. A bigger electrode area lowers the current density needed for a given hydrogen output, but the plates still have to fit the housing and the reservoir. The 5-litre reservoir was sized to fully submerge both electrodes and the pump inlet for a full test run while keeping the whole thing bench-top and portable — output is governed by electrode area and current, not electrolyte volume, so there was no benefit to going bigger. The 8 W pump was picked to clear bubbles from the electrode surfaces without drawing much power itself, and the variable DC supply (up to roughly 22–23 A at 12 V) let us adjust both voltage and current during testing while staying inside the 3–12 V per-electrode safety range.

Table 2. Reproducibility parameters for the HHO Generator cell and test protocol.

Parameter	Value	Basis / Note
Electrolyte composition	Aqueous NaOH, ~30 wt% (70:30 v/v tap water : NaOH stock)	Recorded in build documentation; used consistently throughout.
Electrolyte volume (circulating)	5 L (reservoir capacity)	Full reservoir volume; cell-internal electrolyte volume was not separately measured.
Bipolar plate material / thickness	SS-316L, thickness not independently confirmed in records	[Information Required] — to be measured directly from a spare plate and reported in the next revision.
Plate footprint (per electrode)	160 mm × 160 mm octagonal bounding envelope	From CAD/assembly drawings.
Approximate active electrode area	~210 cm^2 per plate face (geometric estimate)	Calculated from the regular-octagon area inscribed in a 160 × 160 mm square; not independently verified by direct measurement, and does not subtract the two flow-hole openings.
Electrode (inter-plate) spacing	Not recorded	[Information Required] — comparable home-built alkaline cells in the literature report spacings in the 3–8 mm range [15], [19]; the exact value used here should be measured from the physical stack or design drawing and reported.
Number of cells in stack	Multi-plate bipolar stack (exact count not logged)	[Information Required] — visually countable from Figure 9; should be confirmed and stated explicitly.
Operating temperature	Ambient (not logged)	[Information Required] — no thermocouple or temperature log was part of the original test protocol.
Duration of each experimental run	Not recorded precisely	[Information Required] — sufficient to reach the steady 0.01 L/s reading reported in, but exact run length in minutes was not logged.

Operating-point justification (added in this revision). The 12 V, 22 A condition characterised in Section 4 was not chosen from a characterised optimum; rather, it represents the upper end of the safe operating current established during commissioning for this electrode area and O-ring compression. It is also the point at which pump-driven bubble clearance was visually confirmed to keep pace with gas evolution without flooding the gas–water separator. A full voltage–current sweep across the 3–12 V per-electrode envelope was not carried out on the tested build; the single operating point reported in Section 4 should therefore be read as a demonstrated safe operating condition rather than a characterised efficiency optimum. A systematic sweep (e.g., in ≈2 V or ≈5 A increments, while holding electrolyte concentration and temperature fixed), following the design used for comparable small electrolysers [23], [24] is identified as a priority for future work.

Component Photographs:

Figures 2 through 6 show the individual components as fabricated and installed, before final assembly into the complete system.

The DC power supply is a rainproof, variable-output unit rated 12 V and up to roughly 22–23 A, fitted with an integrated digital display that reads out voltage and current in real time so the operating point could be set and monitored directly at the source (Figure 2).

Figure 2. DC Power Supply Unit

Figure 3. Hydrogen Storage Cylinder

Hydrogen produced at the cathode is collected in a low-pressure storage cylinder, secured to the frame with steel retaining bands and fitted with a pneumatic quick-connect fitting at the top for the incoming gas line (Figure 3).

Before hydrogen reaches storage, it passes through a gas–water separator — a sealed cylindrical vessel with an internal collection tube and two pneumatic through-fittings for the inlet and outlet lines, which lets entrained electrolyte droplets settle out under gravity (Figure 4).

Figure 4. Gas–Water Separator

Figure 5. Electrolyte Reservoir with Circulation Pump

The electrolyte reservoir houses the submersible circulation pump directly inside it, with the pump's positive-terminal lead routed out through the lid; this is also where the NaOH solution is mixed and topped up between runs (Figure 5).

An in-line flow-control fitting, spliced into the tubing between the reservoir and the separator, is used to throttle electrolyte flow and balance circulation across the loop (Figure 6). Moreover, the 3D view of the HHO generator cell is shown in Figure 7.

Figure 6. Electrolyte Flow-Control Fitting

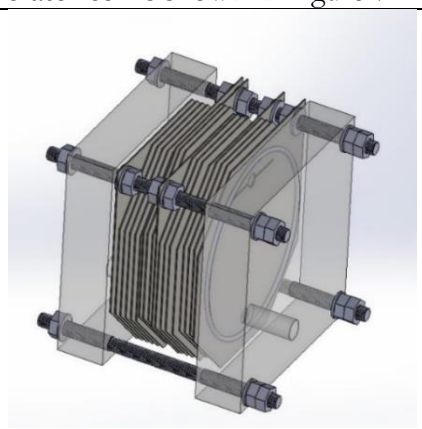

Figure 7. 3D Assembled CAD View of the HHO Generator Cell

Experimental Setup:

Cell Design:

The cell itself is a stack of octagonal SS-316L bipolar electrode plates sandwiched between two transparent acrylic end plates, 160.00 mm × 160.00 mm, held together by four corner threaded rods, with the finished stack coming out to 154.02 mm tall overall. O-ring gaskets sit at every electrode interface and at both end-plate faces, and the four-rod arrangement was chosen specifically so the compressive load spreads evenly across the stack — uneven compression is the fastest way to get a leak. Acrylic was selected for the end plates for three reasons: it is stiff enough to hold the stack under compression, it electrically isolates the two terminal electrodes from each other and from the frame, and it is transparent, so you can actually watch gas evolving inside the cell during a test allowing direct visual observation of gas evolution. Individual plate thickness and exact inter-electrode spacing were not independently logged during fabrication and are listed as open items in Table 2.

Two versions of the bipolar plate appear in the stack: a plain plate with two circular through-holes that act as electrolyte inlet/outlet channels between adjacent cells, and a ported plate with an extra side port for the external electrolyte/gas connection, which shifts its flow-hole layout off-center relative to the plain design. Figure 8 shows the CAD assembly used to verify this design before fabrication.

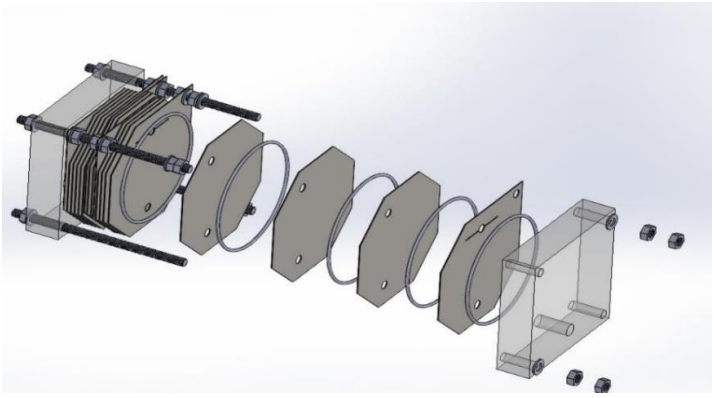

Figure 8. Exploded Assembly View of the Electrode Stack

Figure 9 shows the finished electrode stack as built, with the SS-316L bipolar plates clamped between the acrylic end plates. The hand-marked orientation and hole labels visible on the top plate were added during assembly to keep track of plate stacking order and were not part of the original design.

Figure 9. Fabricated Electrode Stack

Fabrication Sequence:

Fabrication ran from February to June 2026 in the Mechanical Engineering Workshop, and broke down into seven stages that followed on from each other fairly naturally: procuring materials and checking them against the CAD design; machining the octagonal SS-316L plates and the acrylic end plates, including flow-channel drilling and surface polishing; assembling the stack with O-ring gaskets at every joint, tightened crosswise so the compression stayed even; installing the circulation subsystem — reservoir, pump, hoses — and running an initial test with plain water before any electrolyte went near it; assembling the gas–water separator and storage tank, with every gas-side joint checked for leaks using soap water; wiring the DC supply to the cell terminals with polarity and insulation checks, plus a bench test of the pump and pressure gauge; and finally, commissioning the complete system with the full NaOH electrolyte mixture, adjusting flow rate and sealing as needed before we started taking formal measurements. Figure 10 shows the fully assembled system from above, and Figure 11 shows the complete test bench, including the graduated cylinder used for the water-displacement measurement described.

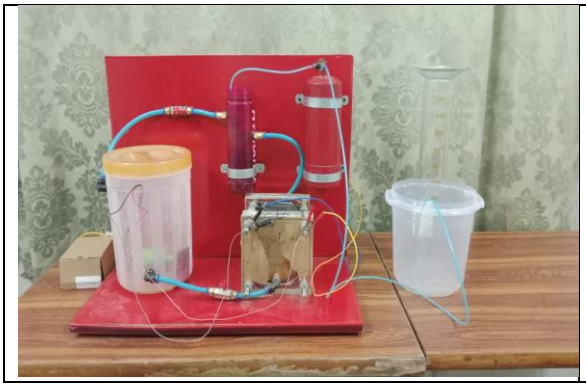

Figure 10. Fully Assembled HHO Generator System

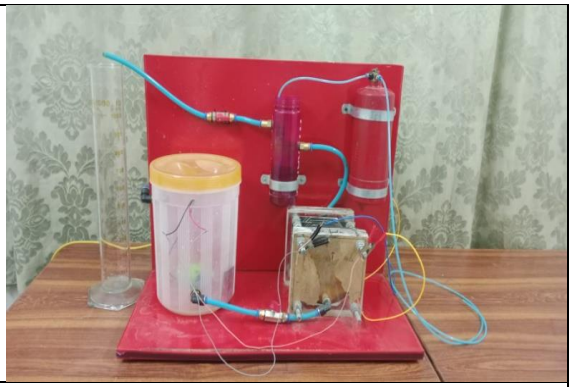

Figure 11. Complete Experimental Test Bench

Hydrogen Flow Measurement:

Hydrogen output was measured by water displacement (shown in Figure 12), which is about as simple as gas-flow measurement gets and does not need any specialized flow-metering equipment. With the DC supply connected across the cell terminals, hydrogen evolving at the

cathode was carried by a gas tube to the lower opening of a graduated cylinder that had been pre-filled with water and inverted, open end down, inside a water-filled vessel — so no air pocket was sitting in the cylinder before the run started. As hydrogen entered from below, it pushed water out of the cylinder in direct proportion to the volume of gas collected, and we read that displaced volume off the cylinder's calibrated scale at fixed time intervals under constant voltage and current. The production rate follows directly from that:

Hydrogen Production Rate (mL/min) = Volume of Hydrogen Collected (mL) / Time Elapsed (min) (1)

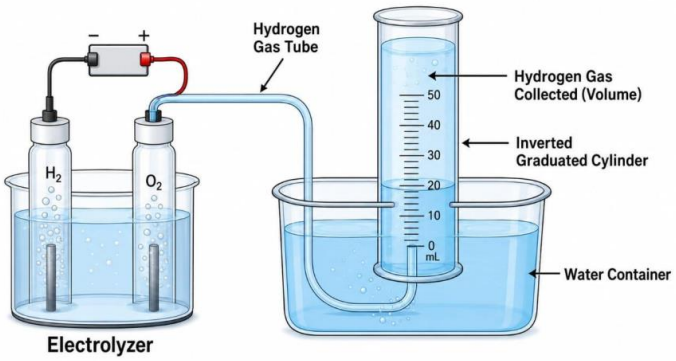

Figure 12. Water-Displacement Measurement Setup

As noted in Table 2 and in the Abstract, this measurement reflects a single run at one fixed operating point; the run duration, cylinder graduation resolution, and timing method were not logged with enough precision in the underlying records to support a formal propagated-uncertainty estimate, and we report this as an explicit limitation rather than an inferred error bar.

Operating Condition and Safety:

Every result comes from the HHO Generator running at a fixed 12 V, 22 A DC input. Before any of that testing started, a hazard assessment covering electrical, fire/explosion, pressure, chemical, and gas-leakage risks turned up sixteen distinct hazards — eight rated medium risk, the rest low risk, and none rated high risk once the specified controls were actually in place. PPE requirements were straightforward: safety goggles, a lab coat, chemical- and heat-resistant gloves, closed shoes, and a face mask, alongside written procedures for electric shock, hydrogen fire response (dry-powder or CO_2 extinguisher only — never water), and gas-leak response.

Measurement Uncertainty Considerations:

The hydrogen-production and efficiency figures reported are for a single run at the 12 V, 22 A operating point; the underlying project records do not include repeated trials or a logged estimate of measurement uncertainty. Rather than attach an invented ± value to that single reading, this section sets out the principal sources of error in the water-displacement method used so that they can be budgeted for in the repeated-trial campaign recommended, following the propagation approach used for comparable small-scale electrolyser rigs [23].

Table 3 shows four sources are expected to dominate. (1) Reading resolution: graduated cylinders of the class used here typically carry divisions equivalent to a few percent of the collected volume per reading, so meniscus-reading error alone is a plausible percent-level contributor. (2) Timing resolution: manual timing of the displacement interval carries an uncertainty of the order of a second per reading, which matters more at short collection intervals than long ones. (3) Water-vapour content: hydrogen collected over water is saturated with water vapour at the ambient temperature, and the reported 0.01 L/s was not corrected to a dry-gas, standard-temperature-and-pressure (STP) basis; without that correction the measured volume is a systematic over-estimate of the dry hydrogen actually produced, typically

by a few percent near room temperature. (4) Undetected leakage. The records document a soap-water leak check during fabrication, but no dedicated leak-rate measurement during the timed run itself, so a small, unquantified gas loss between the cell and the collection cylinder cannot be ruled out. Ambient temperature and pressure were not logged during the timed run, so no STP correction could be applied after the fact.

Table 3. Indicative sources of measurement error in the water-displacement method (qualitative; no repeated trials were recorded for this build, so no numerical uncertainty is claimed for the reported 0.01 L/s).

Error source	Nature of effect	Recommended mitigation
Graduated-cylinder reading resolution	Random; shrinks with averaging over repeated trials	Repeat each condition 3–5 times; report mean ± SD
Manual timing resolution	Random; larger at short collection intervals	Use longer collection windows or automated timing
Water-vapour content of collected gas	Systematic over-estimate of dry H_2 volume	Apply STP/dry-gas correction using logged bath temperature and ambient pressure, as in [23]
Undetected tubing/fitting leakage	Systematic under- or over-estimate depending on leak location	Run a zero-current blank test to bound the leak rate
Ambient temperature/pressure drift	Small systematic effect on STP-corrected volume	Log temperature and pressure throughout each run

Results:

Hydrogen Production Rate:

At 12 V and 22 A, the system settled into a steady hydrogen output of

$$Q(H_2) = 0.01 \text{ L/s} = 0.6 \text{ L/min} = 36 \text{ L/h} \quad (2)$$

and held that figure for the rest of the test, which is a reasonable sign that the system had actually reached steady state rather than still ramping up or trailing off. Given that the electrodes carry no catalyst coating at all, this output sits about where you would expect for bare stainless steel in an alkaline electrolyte — nobody involved in the build was expecting catalyst-grade performance from uncoated SS-316L, and the numbers reflect that.

Power Consumption and Efficiency:

Electrical input power follows directly from Ohm's power law:

$$P_{in} = V \times I = 12 \text{ V} \times 22 \text{ A} = 264 \text{ W} \quad (3)$$

and that 264 W does not all go toward splitting water. Table 4 breaks down where the rest of it goes.

Table 4. Electrochemical and electrical loss mechanisms in the electrolysis system.

Loss mechanism	Description
Electrochemical activation energy	Water splitting only starts once the applied voltage clears the 1.23 V theoretical decomposition threshold; on a bare, uncoated SS-316L surface, the activation overpotential needed to actually drive the reaction is higher still, and that extra voltage is paid for in extra input power.
Ohmic resistance of the electrolyte	As hydroxide ions migrate through the NaOH electrolyte from cathode to anode, they run into ionic resistance, and the energy that resistance dissipates comes out as heat rather than hydrogen.
Plate and contact resistance	Electrical resistance at the interfaces between the stainless-steel plates and the current-carrying connections is small individually, but it adds up across the whole stack and current path.

Using the lower heating value of hydrogen at standard low-pressure lab conditions,
$LHV = 10.8\ kJ/L$
the hydrogen energy output rate comes out to

$$P_{out} = Q(H_2) \times LHV = 0.01\ L/s \times 10.8\ kJ/L = 108\ W \quad (4)$$

which gives an overall efficiency of

$$\eta = (P_{out} / P_{in}) \times 100 = (108 / 264) \times 100 \approx 41\% \quad (5)$$

That leaves 156 W — roughly 59% of the input — that never shows up as hydrogen chemical energy. Table 5 lists where it actually goes, beyond the electrochemical and ohmic losses already covered in Table 4.

Table 5. Additional energy loss pathways affecting system efficiency.

Loss mechanism	Description
Gas bubble accumulation	Hydrogen and oxygen bubbles that stick to the electrode faces block part of the active reaction area, which raises the effective resistance the current has to push through.
Thermal dissipation	General heat loss from the electrolyte and the cell body to the surroundings over the course of sustained operation.
System leakage and flow resistance	Small energy losses from resistance in the gas lines and minor leakage points around the circulation loop.

Comparison with Commercial and Recent Low-Cost Systems:

Table 6 sets the measured 41% against representative commercial alkaline and PEM systems, and against the recent low-cost alkaline/HHO generator.

Table 6. Benchmark performance comparison.

System	Catalyst / electrode type	Cell efficiency	Notes
Industrial commercial AWE	Nickel foam / cobalt-based	65–75%	Optimized commercial system
Advanced commercial PEM	Platinum / iridium	70–82%	Optimized commercial system
[19]	SS-316L, 136.5 cm^2, 4 mm spacing	69.3%	Best point from a KOH/NaOH concentration sweep
[20]	SS-316L, optimized wet-cell	59.74%	Best of four configurations tested
This work – HHO Generator	Bare SS-316L (no catalyst)	~41%	Single fixed operating point, no optimization sweep

The gap between this result and the two most recent comparable studies is consistent with the difference in approach: both [19] and [20] report the best point from a deliberate optimization sweep across electrode geometry and/or electrolyte concentration, while this work reports a single fixed condition on a first-build system that has not yet been optimized in the same way.

Additional Performance Indicators:

Beyond the LHV energy efficiency, four further indicators can be computed directly from the single recorded operating point (12 V, 22 A, $Q(H_2)$ = 0.01 L/s) without any additional measurement. The Faradaic efficiency calculation below assumes the stack behaves as N = 6 electrically series-connected cells, consistent with the as-built configuration of 18 plates and 6 electrode connections communicated by the authors; because the exact internal series/parallel wiring was not recorded in the original build documentation — and Table 2 likewise flags the exact cell count as an open item — this value should be verified against the as-built wiring diagram before it is finalised for publication. Table 7 demonstrates the additional performance indicators derived from the 12 V, 22 A operating point

The theoretical hydrogen volume at 100% Faradaic efficiency follows from Faraday's second law, $V(H_2,theor) = N \cdot I / (2F) \cdot V_m$, where F is the Faraday constant (96 485 C/mol) and V_m is the molar volume implied by the LHV value already used in Eq. (4) (22.4 L/mol). For N = 6 and I = 22 A this gives $V(H_2,theor) \approx 0.0153$ L/s, against the measured 0.01 L/s, i.e. a Faradaic efficiency of ≈ 65%.

Table 7. Additional performance indicators derived from the 12 V, 22 A operating point.

Indicator	Value	Basis/assumption
Faradaic efficiency	≈ 65%	N = 6 series cells (author-confirmed plate count); Faraday's law
Current density	≈ 0.086 A/cm² (860 A/m²)	Gross 160×160 mm plate area; through-hole area not netted out, so this is a lower-bound estimate
Specific energy consumption	≈ 81 kWh/kg H_2 (≈ 7.3 kWh/Nm³)	Pin/mass or volume of H_2 produced; consistent with the 41% LHV efficiency in Eq. (5)
H_2 yield per unit electrical energy	≈ 136 L/kWh	$Q(H_2)$ / Pin
Production stability	Qualitatively steady over the single run	Run duration/sampling interval not logged; quantitative drift analysis not available

The Faradaic efficiency (≈65%) is markedly higher than the 41% LHV energy efficiency, and this gap is expected rather than anomalous: Faradaic efficiency measures only how much of the applied current drives the water-splitting half-reactions rather than parasitic side-reactions, whereas the LHV efficiency also carries the activation-overpotential penalty of running an uncoated SS-316L electrode (Table 4). Read together, the two numbers indicate that most of the applied current is in fact doing useful electrochemical work, and that the shortfall relative to commercial catalysed systems (Table 6) is concentrated in the voltage the cell needs to drive that current, not in stray or leakage current — which is consistent with the catalyst-coating recommendation and with the general pattern reported for uncatalysed versus catalysed alkaline electrodes elsewhere [21], [22], [25]. The estimated current density (≈0.09 A/cm²) is well below the ≈0.1–0.4 A/cm² range typical of engineered small alkaline stacks [3], [24], consistent with the large-electrode, low-current-density design choice.

Cost Analysis and Bill of Materials:

Table 8 itemises the components priced by the authors for the tested build, in Pakistani Rupees (PKR). The DC power supply and the pressure gauge/flow indicator listed in Table 1 were not priced separately in the project records supplied for this revision and are flagged below as a gap to close before this table is treated as a complete bill of materials.

Table 8. Bill of materials for the tested HHO Generator build

Component	Quantity / basis	Cost (PKR)
Electrolyte reservoir	1	800
DC circulation pump	1	500
Gas–water separator bottle	1	450
Hydrogen storage tank	1	5,000
Connecting hose/tubing (all)	lot	1,000
Flow-control valves and attachment nuts	lot	4,000
SS-316L sheet stock	4 kg @ PKR 6,000/kg	24,000
O-ring seals	18 @ PKR 100	1,800
Nuts and bolts (fasteners)	lot	1,500

Subtotal, itemised components		39,050
Labour, travel, workshop setup and miscellaneous	reported total less itemised components	30,950
Total reported project cost		70,000

At the prevailing interbank rate of ≈278 PKR/USD (August 2026), the PKR 70,000 total corresponds to approximately USD 252, and the itemised component subtotal of PKR 39,050 to approximately USD 140; both figures exclude the DC power supply. For context, recent techno-economic reviews put commercial alkaline electrolyser capital cost at roughly USD 800/kW as of 2024, trending toward USD 600/kW for PEM systems by 2030 [26], [27], which for a unit of this electrical rating (264 W) implies an equivalent engineered-hardware cost on the order of USD 170–210 once scaled down, excluding balance-of-plant, installation, and the catalyst coating and precision manufacturing that this bench-built, uncoated prototype does not attempt to replicate. This comparison is illustrative rather than like-for-like: the commercial figure is a scaled $/kW capital-cost benchmark for warrantied, catalysed hardware, while the PKR 70,000 figure includes labour and travel for a single hand-built unit but excludes the power supply. A rigorous low-cost claim would require completing the bill of materials with the missing power-supply and instrumentation costs and comparing both systems on the same basis (e.g. USD/kW or USD per litre of H_2 produced per day) rather than on total build cost alone.

Discussion:

A 41% efficiency is well below the 65–75% typical of industrial AWE and the 70–82% typical of PEM, and Table 5 makes the reason fairly obvious: the commercial benchmarks use catalysts — nickel foam or cobalt coatings for AWE, platinum and iridium for PEM — that cut the activation overpotential at the electrode surface, while this build runs on bare SS-316L with nothing on it [4], [5]. It is also below the two most comparable recent low-cost studies, [19] and [20], both of which optimized electrode configuration or electrolyte concentration before reporting their best number; this system has not yet gone through that kind of sweep. None of this is really a surprise — it is close to what you would predict from skipping both the catalyst step and the optimization step — and none of the three loss mechanisms in Tables 3 and 4 are unusual for alkaline electrolysis generally; they show up in commercial and research-grade units too, just suppressed by design choices this build has not yet made. The electrode-spacing and bubble-blocking effects in particular have been characterized experimentally in home-built alkaline cells directly comparable to this one [15], [21], [22].

The result does support a narrower claim: a hydrogen-generation system built entirely from parts available in Pakistani markets, assembled with ordinary workshop tools, can run continuously and produce a measurable and steady hydrogen output as a complete integrated system — not just an isolated electrode pair. That is a different achievement from matching commercial or research-optimized efficiency, and this was the primary purpose of the prototype. Measured against the ten objectives, six were addressed directly — a working system was designed and built from local materials, its voltage–current behavior and hydrogen output were characterized, its efficiency was calculated, and start-up/shutdown procedures were established and followed. The remaining four — catalyst-coating work, deeper study of the circulation and separation dynamics, market analysis, and the broader knowledge-base contribution — are the natural next steps rather than gaps in this particular test.

A few limitations in the underlying data should be acknowledged rather than glossing over. As stated in the Abstract, Table 2, and the production-rate and efficiency figures here come from a single measurement run at a single operating point (12 V, 22 A); no repeat trials were performed, and no formal measurement uncertainty was propagated, because the underlying instrument-resolution and timing data needed to do so honestly were not logged

with sufficient precision. A full voltage–current sweep across a range of conditions, of the kind Gad et al. and Fayez et al. both performed [19], [20], would give a much more complete picture of how efficiency actually changes with load, and is identified as the highest priority.

On electrolyte composition specifically: NaOH, at approximately 30 wt% (70:30 v/v tap water to NaOH), is the electrolyte used throughout the system described in this paper, consistently, and in every calculation. An earlier internal draft of this manuscript contained one stray reference to "KOH electrolyte solution" in this Discussion section; that was a drafting error, not a record of a different electrolyte actually used in the reported test, and it has been removed and corrected here. No electrolyte-related value, calculation, or result in this paper depends on that earlier error, and none has been changed as a result of this correction — only the inconsistent wording has.

The DC-supply rating discrepancy (17.5 A on the component list versus 22 A used for the results) is a separate, genuine open item: it does not affect the physics of what was measured, since the reported results are all calculated from the 22 A test condition, but the supply's true rated capacity should be re-confirmed against its nameplate before this work is extended or resubmitted elsewhere.

This revision adds several analyses requested in a second round of review shows that, although the LHV energy efficiency of 41% is modest, the estimated Faradaic (charge) efficiency is considerably higher at ≈65%, indicating that most of the applied current is in fact driving the water-splitting reaction and that the shortfall relative to catalysed commercial systems is concentrated in voltage overpotential rather than in parasitic current losses — a distinction that matters for prioritising the catalyst-coating work recommended puts a first real cost figure on the claimed low-cost advantage: at roughly USD 250 total (excluding the DC power supply), the build sits one to two orders of magnitude below scaled commercial capital-cost benchmarks, though a rigorous cost-advantage claim still requires completing the bill of materials and comparing both systems on a consistent USD/kW or USD-per-litre basis. Neither addition changes the central finding already stated above: with a single operating point and no repeated trials, the reported 41% efficiency and 0.01 L/s production rate should be read as a demonstrated proof-of-operation figure, not as a statistically characterised performance envelope.

Conclusion:

We built a low-cost HHO Generator around alkaline water electrolysis, using materials sourced entirely within Pakistan and standard workshop fabrication — no imported cell stacks, no specialized coating equipment. The finished system, with its SS-316L bipolar electrode stack, closed-loop NaOH circulation, gas–water separation, and low-pressure hydrogen storage, was modeled in SolidWorks before any of it was physically built, mainly to catch fit and sealing problems early. Running at a regulated 12 V, 22 A DC input, it produced hydrogen steadily at 0.01 L/s (0.6 L/min), taking in 264 W of electrical power to yield 108 W of hydrogen chemical energy — an overall efficiency of 41%, measured in a single test run at this one operating point. That number sits below commercial alkaline (65–75%) and PEM (70–82%) systems, and below the two most comparable recent low-cost alkaline/HHO studies in the literature (59.74–69.3%) [19], [20], which is consistent with this being a first-generation, single-configuration prototype running on bare, uncatalyzed electrodes with no optimization sweep performed. It confirms that low-cost, laboratory-scale green hydrogen production is technically workable, and it gives a fully documented, honestly limited baseline.

Taking this forward, the most direct next step is adding a catalyst — Ni–Fe alloy or nickel-foam coatings on the electrodes should meaningfully cut the activation losses without touching the rest of the design. Beyond that, we would want to see the system run on solar PV with proper MPPT to remove its dependence on grid electricity, a full voltage–current and electrolyte-concentration sweep with repeated trials and reported measurement uncertainty to

replace the single-point characterization used here, tighter sealing and gasket materials for sustained alkaline exposure, and a move from low-pressure collection to compressed or purified storage once the electrode-side improvements are in place. None of this changes what the current build already shows: that a working, continuously operating hydrogen generator can be developed on a limited budget, and that it is a workable platform for both further catalyst and design research and for teaching electrochemical energy conversion to the next group of students who pick this up.

Recommendations:

The limitations identified point to the following concrete next steps, each linked to the gap it addresses.

Repeated-trial testing and statistical characterisation. The present dataset is a single run at one operating point; the immediate priority is to repeat the 12 V/22 A test 3–5 times and report the mean and standard deviation of $Q(H_2)$ and η, using the uncertainty budget.

Voltage–current sweep. The operating point was set by the safety envelope established during commissioning, not by a characterised optimum; a systematic sweep across the 3–12 V per-electrode range at fixed electrolyte concentration and temperature is needed to locate the efficiency-optimal window, following designs such as [23], [24].

Catalyst-coated electrodes. Attribute most of the efficiency gap with commercial systems to the bare SS-316L surface; a Ni–Fe or nickel-foam coating is the highest-leverage single change available without redesigning the cell [28], [25].

Optimised electrode spacing. Bubble-blocking losses (Table 3) are geometry-sensitive [29]; therefore, spacing should be varied alongside the voltage–current sweep above — the exact spacing used in the current build is itself an open item flagged in Table 2.

Renewable/solar power integration. Replacing the grid-connected DC supply with a PV/MPPT source, as demonstrated at comparable scale elsewhere, would align the build with its stated green-hydrogen motivation.

Gas purification and storage. The current low-pressure store has no purification stage; a small pressure-swing-adsorption or scrubbing stage [30], [31] would be needed before the hydrogen could be used in any application sensitive to moisture or electrolyte carryover.

Extended-duration testing. Production stability (Table 7) was assessed only qualitatively over a single run; multi-hour logging is needed to distinguish true steady-state operation from slow drift.

Complete cost accounting. The bill of materials excludes the DC power supply and gauges; closing this gap is a prerequisite for any quantitative low-cost claim relative to commercial systems.

Close the remaining open build-record items. Table 2 flags plate thickness, electrode spacing, cell count, operating temperature, and run duration as not independently confirmed; these should be measured directly from the physical prototype ahead of any further submission, alongside the DC-supply nameplate re-check.

Nomenclature:

Symbol	Description	Unit
V	Operating voltage across the HHO Generator terminals	V
I	Operating current	A
P_{in}	Electrical input power (V × I)	W
$Q(H_2)$	Volumetric hydrogen production rate	L/s, L/min
LHV	Lower heating value of hydrogen	kJ/L
P_{out}	Hydrogen energy output rate ($Q(H_2)$ × LHV)	W
η	Overall system efficiency (P_{out} / P_{in} × 100)	%

F_e	Faradaic efficiency ($Q(H_2)$actual / $Q(H_2)$theoretical × 100)	%
J	Current density (I / electrode area)	A/cm²
SEC	Specific energy consumption (Pin per unit mass or volume of H_2)	kWh/kg, kWh/Nm³
Y	Hydrogen yield per unit electrical energy ($Q(H_2)$ / Pin)	L/kWh
N	Assumed number of electrically series-connected cells in the stack	–

References:

[1] I. Dincer and C. Acar, "Review and evaluation of hydrogen production methods for better sustainability," *Int. J. Hydrogen Energy*, vol. 40, no. 34, pp. 11094–11111, Sep. 2015, doi: 10.1016/J.IJHYDENE.2014.12.035.

[2] I. Staffell *et al.*, "The role of hydrogen and fuel cells in the global energy system," *Energy Environ. Sci.*, vol. 12, no. 2, pp. 463–491, Feb. 2019, doi: 10.1039/C8EE01157E.

[3] T. T. Jörn Brauns, "Alkaline Water Electrolysis Powered by Renewable Energy: A Review," *Processes*, vol. 8, no. 2, p. 248, 2020, doi: https://doi.org/10.3390/pr8020248.

[4] M. Carmo, D. L. Fritz, J. Mergel, and D. Stolten, "A comprehensive review on PEM water electrolysis," *Int. J. Hydrogen Energy*, vol. 38, no. 12, pp. 4901–4934, Apr. 2013, doi: 10.1016/J.IJHYDENE.2013.01.151.

[5] C. Minke, M. Suermann, B. Bensmann, and R. Hanke-Rauschenbach, "Is iridium demand a potential bottleneck in the realization of large-scale PEM water electrolysis?," *Int. J. Hydrogen Energy*, vol. 46, no. 46, pp. 23581–23590, Jul. 2021, doi: 10.1016/J.IJHYDENE.2021.04.174.

[6] D. Hua, J. Huang, E. Fabbri, M. Rafique, and B. Song, "Development of Anion Exchange Membrane Water Electrolysis and the Associated Challenges: A Review," *ChemElectroChem*, vol. 10, no. 1, p. e202200999, Jan. 2023, doi: 10.1002/CELC.202200999;SUBPAGE:STRING:FULL.

[7] D. S. Falcão, "Green Hydrogen Production by Anion Exchange Membrane Water Electrolysis: Status and Future Perspectives," *Energies 2023, Vol. 16, Page 943*, vol. 16, no. 2, p. 943, Jan. 2023, doi: 10.3390/EN16020943.

[8] I. Vincent and D. Bessarabov, "Low cost hydrogen production by anion exchange membrane electrolysis: A review," *Renew. Sustain. Energy Rev.*, vol. 81, pp. 1690–1704, Jan. 2018, doi: 10.1016/J.RSER.2017.05.258.

[9] M. A. Laguna-Bercero, "Recent advances in high temperature electrolysis using solid oxide fuel cells: A review," *J. Power Sources*, vol. 203, pp. 4–16, Apr. 2012, doi: 10.1016/J.JPOWSOUR.2011.12.019.

[10] "Water Electrolysis - an overview | ScienceDirect Topics." Accessed: Aug. 29, 2026. [Online]. Available: https://www.sciencedirect.com/topics/engineering/water-electrolysis

[11] O. Schmidt, A. Gambhir, I. Staffell, A. Hawkes, J. Nelson, and S. Few, "Future cost and performance of water electrolysis: An expert elicitation study," *Int. J. Hydrogen Energy*, vol. 42, no. 52, pp. 30470–30492, Dec. 2017, doi: 10.1016/J.IJHYDENE.2017.10.045.

[12] G. Sakas, A. Ibáñez-Rioja, V. Ruuskanen, A. Kosonen, J. Ahola, and O. Bergmann, "Dynamic energy and mass balance model for an industrial alkaline water electrolyzer plant process," *Int. J. Hydrogen Energy*, vol. 47, no. 7, pp. 4328–4345, Jan. 2022, doi:

10.1016/J.IJHYDENE.2021.11.126.

[13] U. K. Mirza, N. Ahmad, K. Harijan, and T. Majeed, "Identifying and addressing barriers to renewable energy development in Pakistan," *Renew. Sustain. Energy Rev.*, vol. 13, no. 4, pp. 927–931, May 2009, doi: 10.1016/J.RSER.2007.11.006.

[14] S. A. M. Irfan Ahmad Gondal, "Green hydrogen production potential for developing a hydrogen economy in Pakistan," *Int. J. Hydrogen Energy*, vol. 43, no. 12, pp. 6011–6039, 2018, [Online]. Available: https://www.sciencedirect.com/science/article/abs/pii/S0360319918302258

[15] P. C. Okonkwo, H. Bhowmik, I. B. Mansir, M. A. A. Al Sarj Al Marhoon, and N. F. A. Al Sfarini, "Effect of electrode spacing on hydrogen production using a home-made alkaline electrolyzer," *Mater. Lett.*, vol. 306, p. 130841, Jan. 2022, doi: 10.1016/J.MATLET.2021.130841.

[16] P. C. Okonkwo, E. M. Barhoumi, I. B. Mansir, W. Emori, and H. Bhowmik, "Effect of electrode material on the hydrogen production using a low-cost home-made alkaline electrolyzer," *Vacuum*, vol. 198, p. 110878, Apr. 2022, doi: 10.1016/J.VACUUM.2022.110878.

[17] L. Bunge, H. G. Silva, P. L. Cruz, and M. Iten, "Testing of a Low-Cost Dry Cell Prototype for Oxyhydrogen Production," *Designs*, vol. 6, no. 5, p. 79, Oct. 2022, doi: 10.3390/DESIGNS6050079/S1.

[18] A. M. Mousa, H. A. A. Sayed, K. A. M. Ali, N. S. Elkaoud, and W. A. E. Mahmoud, "Energy-conversion efficiency for producing oxy-hydrogen gas using a simple generator based on water electrolysis," *Sci. Rep.*, vol. 14, no. 1, Dec. 2024, doi: 10.1038/S41598-024-73534-1.

[19] M. S. Gad, A. K. El Soly, S. Singh, K. Sharma, S. Dixit, and M. irfanul H. Siddiqui, "Examining oxyhydrogen gas generation experimentally using wet cell design," *PLoS One*, vol. 20, no. 6, p. e0324921, Jun. 2025, doi: 10.1371/JOURNAL.PONE.0324921.

[20] N. H. A. Fayez, M. Qenawy, H. M. M. Mustafa, M. Shehadeh, M. Taha, and A. H. Abdelbaky Elbatran, "Optimization of a wet-cell electrolyzer for efficient oxyhydrogen (HHO) gas production: a step towards sustainable green energy solutions," *Sci. Reports 2026 161*, vol. 16, no. 1, pp. 12374-, Apr. 2026, doi: 10.1038/s41598-026-45418-z.

[21] A. Lasia, "Mechanism and kinetics of the hydrogen evolution reaction," *Int. J. Hydrogen Energy*, vol. 44, no. 36, pp. 19484–19518, Jul. 2019, doi: 10.1016/J.IJHYDENE.2019.05.183.

[22] C. C. L. McCrory, S. Jung, J. C. Peters, and T. F. Jaramillo, "BenchmarkingHeterogeneous Electrocatalysts for theOxygen Evolution Reaction," *J. Am. Chem. Soc.*, vol. 135, no. 45, pp. 16977–16987, Nov. 2013, doi: 10.1021/JA407115P.

[23] N. Mostafa, H. Emad, M. Eltaweel, and M. Chizari, "Statistical Analysis of the Operating Conditions Influencing Green Hydrogen Production by a Reversible PEM Water Electrolyser," *Process. 2026, Vol. 14, Page 2661*, vol. 14, no. 16, p. 2661, Aug. 2026, doi: 10.3390/PR14162661.

[24] L. Rabillard *et al.*, "Experimental Investigation of two low-cost 5 kW alkaline electrolyzer prototypes' performances depending on size and applied voltage," *Int. J. Hydrogen Energy*, vol. 125, pp. 100–107, May 2025, doi: 10.1016/J.IJHYDENE.2025.03.418.

[25] P. A. Kempler and A. C. Nielander, "Reliable reporting of Faradaic efficiencies for electrocatalysis research," *Nat. Commun. 2023 141*, vol. 14, no. 1, pp. 1158-, Mar. 2023, doi: 10.1038/s41467-023-36880-8.

[26] E. N. Aminaho, N. S. Aminaho, and F. Aminaho, "Techno-economic assessments of

electrolyzers for hydrogen production," *Appl. Energy*, vol. 399, p. 126515, Dec. 2025, doi: 10.1016/J.APENERGY.2025.126515.

[27] S. Mushtaq *et al.*, "Sustainability of green hydrogen: A viewpoint in Pakistan," *Energy Environ.*, vol. 36, no. 2, pp. 1063–1079, Mar. 2025, doi: 10.1177/0958305X251315405;CTYPE:STRING:JOURNAL.

[28] Y. Xia, H. Cheng, H. He, and W. Wei, "Efficiency and consistency enhancement for alkaline electrolyzers driven by renewable energy sources," *Commun. Eng. 2023 21*, vol. 2, no. 1, pp. 22-, May 2023, doi: 10.1038/s44172-023-00070-7.

[29] N. Nagai, M. Takeuchi, T. Kimura, and T. Oka, "Existence of optimum space between electrodes on hydrogen production by water electrolysis," *Int. J. Hydrogen Energy*, vol. 28, no. 1, pp. 35–41, Jan. 2003, doi: 10.1016/S0360-3199(02)00027-7.

[30] M. Luberti and H. Ahn, "Review of Polybed pressure swing adsorption for hydrogen purification," *Int. J. Hydrogen Energy*, vol. 47, no. 20, pp. 10911–10933, Mar. 2022, doi: 10.1016/J.IJHYDENE.2022.01.147.

[31] "ISO/TS 19883:2017 - Safety of pressure swing adsorption systems for hydrogen separation and purification." Accessed: Aug. 31, 2026. [Online]. Available: https://www.iso.org/standard/61169.html

Copyright © by authors and 50Sea. This work is licensed under the Creative Commons Attribution 4.0 International License.